Copy 5
RM E56A17

NACA RM E56A17

NACA

RESEARCH MEMORANDUM

FOR REFERENCE

PERFORMANCE OF SUPERSONIC RAMP-TYPE SIDE INLET WITH COMBINATIONS OF FUSELAGE AND INLET THROAT BOUNDARY-LAYER REMOVAL

By Robert C. Campbell

Lewis Flight Propulsion Laboratory
Cleveland, Ohio

NATIONAL ADVISORY COMMITTEE
FOR AERONAUTICS

WASHINGTON
April 25, 1956

NATIONAL ADVISORY COMMITTEE FOR AERONAUTICS

RESEARCH MEMORANDUM

PERFORMANCE OF SUPERSONIC RAMP-TYPE SIDE INLET WITH COMBINATIONS OF FUSELAGE AND INLET THROAT BOUNDARY-LAYER REMOVAL

By Robert C. Campbell

SUMMARY

An experimental investigation to evaluate combinations of fuselage and inlet throat boundary-layer removal for a ramp-type side inlet was conducted in the Lewis 8- by 6-foot supersonic wind tunnel at Mach numbers 1.5, 1.8, and 2.0.

Optimum combinations of fuselage and inlet throat boundary-layer removal showed gains in available thrust from 3 to 10 percent over the case of no inlet throat bleed and full external fuselage boundary-layer removal. The maximum gains occurred with fuselage boundary-layer diverter heights from zero to one-third of the fuselage boundary-layer thickness. Maximum pressure recoveries at Mach number 2.0 were about 0.91 and at each Mach number appeared comparable for all external diverter heights, provided sufficient bleed area was available. Total-pressure distortions at maximum net thrusts were below 10 percent.

INTRODUCTION

Considerable emphasis has been placed on the desirability of complete, or nearly complete, fuselage boundary-layer removal for side inlets because of the sensitivity of several such inlets to submersion in this boundary layer (refs. 1 to 3). Recent experience with inlets not immersed in the fuselage boundary layer has indicated the beneficial effects of additional boundary-layer removal in the vicinity of the inlet throat (refs. 4 and 5). To date, inlet throat boundary-layer removal has been employed with complete fuselage boundary-layer removal or in very limited combinations with fuselage removal (ref. 6).

In order to determine the optimum combinations of fuselage boundary-layer removal and inlet throat boundary-layer removal, an investigation was conducted in the NACA Lewis 8- by 6-foot supersonic wind tunnel

over a wide range of combinations. A 14° ramp-type side inlet was mounted on a fuselage and run at zero angle of attack at free-stream Mach numbers 1.5, 1.8, and 2.0.

SYMBOLS

A	area
$A_{B,e}$	internal-bleed minimum exit area, sq in.
$A_{B,i}$	internal-bleed minimum inlet area, 4.25 sq in.
A_f	maximum frontal area of basic configuration, 109.3 sq in.
A_i	inlet capture area, 19.51 sq in.
A_t	inlet throat area, 13.55 sq in.
A_2	diffuser flow area at model station 85.0, 22.96 sq in.
C_D	drag coefficient, D/q_0A_f
D	configuration drag, lb
D_a	incremental drag, $D - D_b$, lb
F	internal thrust of turbojet-engine and inlet combination, lb
h	fuselage boundary-layer diverter height, in.
m	mass-flow rate, ρVA, slugs/sec
m_h	theoretical fuselage boundary-layer mass flow diverted
$\frac{m_s}{m_0}$	gross mass-flow ratio spilled, $\frac{m_{3,b} - m_3 + m_h}{m_0}$
m_0	free-stream mass-flow rate, $\rho_0 V_0 A_i$, slugs/sec
$\frac{m_3}{m_0}$	main-duct mass-flow ratio, $\frac{\text{main-duct mass flow}}{\rho_0 V_0 A_i}$
$m_{3,b}$	critical main-duct mass flow of basic configuration
P	total pressure, lb/sq ft
$P_{max} - P_{min}$	maximum total-pressure variation across pressure rakes at model station 85.0

$\frac{P_{max} - P_{min}}{P_2}$	total-pressure distortion
q_0	free-stream dynamic pressure, $\frac{\rho_0 V_0^2}{2}$
t	fuselage boundary-layer thickness, approx. 0.55 in.
V	velocity, ft/sec
$\frac{w\sqrt{\theta}}{\delta A}$	weight flow per unit area, referenced to standard sea-level conditions
δ	ratio of total pressure to NACA standard sea-level total pressure of 2116.22 lb/sq ft
θ	ratio of total temperature to NACA standard sea-level temperature of 518.688° R
ρ	mass density

Subscripts:

b	basic configuration: h/t = 1, no inlet throat bleed (bleed exit closed)
max	maximum
min	minimum
0	free stream
2	diffuser total-pressure survey station, model station 85.0
3	diffuser static-pressure survey station, model station 99.2

APPARATUS AND PROCEDURE

Details of the fuselage, inlet, and boundary-layer removal systems are illustrated in figure 1, and photographs of the model appear in figure 2. A 14° ramp-type inlet was mounted on the flat under side of a basic body of revolution consisting of an ogive nose and a 10-inch-diameter cylindrical afterbody aft of model station 46.2. The inlet cowl lip was located at model station 61.9. Swept side fairings on the inlet extended from the cowl sides to the leading edge of the ramp.

[redacted]

Fuselage boundary-layer diverter height was varied with a series of 40°-included-angle wedges inserted between the body and the inlet-diffuser installation. The diffuser reference line was maintained parallel to the body axis at all times. The inlet throat boundary-layer removal system consisted of a flush slot on the compression ramp inside the inlet and extended from wall to wall. Dimensions and contours of this slot are detailed in figure 1. Mass flow drawn into this slot was ejected through openings in either side of the inlet cowl. Variations in bleed mass flow were accomplished by varying back pressure in the bleed passage with a pair of remotely controlled doors at the bleed exits. The unbroken contour of the diffuser without the bleed passage is indicated by dashed lines on the schematic drawing of figure 1. The area variation of the smooth-contour diffuser is shown in figure 3.

The model was sting-supported and connected to the sting by several strain-gage balance links that measured normal and axial forces. Inlet mass flow was varied by means of a remotely controlled movable tail-pipe plug attached to the sting.

Pressure instrumentation consisted of a flow-field survey rake ahead of the inlet at model station 55.1, 24 total-pressure tubes plus static-pressure orifices at station 85.0 in the diffuser, static-pressure orifices at station 99.2 in the diffuser, base-pressure orifices, and chamber-pressure orifices located in the model balance cavity. The outermost total-pressure tubes at station 85.0 were located 0.2 inch from the wall (0.894 duct rad.).

Main-duct mass-flow ratio was determined from the static-pressure measurements at station 99.2 and the known area ratio between that station and the exit plug where the flow was assumed to be choked. Average total pressure was calculated by area-weighting the total-pressure measurements. The forces resulting from the change in the momentum of the inlet air from free stream to the diffuser exit, and base forces resulting from the difference in base pressure from free-stream static pressure have been excluded from the model force data. Although the model frontal area decreased with decreasing fuselage diverter height, all model force data are based on the model frontal area for the diverter height equal to the boundary-layer thickness.

The model was tested at zero angle of attack and free-stream Mach numbers 1.5, 1.8, and 2.0 with four external diverter heights ($h/t = 0$, $1/3$, $2/3$, and 1). At each diverter height and Mach number, main-duct mass-flow ratio was varied for several internal-bleed exit areas. Reynolds number varied from 4×10^6 to 5×10^6 per foot. The Mach number ahead of the inlet as determined from the survey rake at station 55.1 was within 0.02 of the free-stream Mach number, and the total fuselage boundary-layer thickness, also determined from this rake, was 0.55 inch at the Mach numbers tested.

RESULTS AND DISCUSSION

Variations of diffuser total-pressure distortion and total-pressure recovery and external drag coefficient are shown in figure 4 as a function of main-duct mass-flow ratio for all combinations of fuselage and inlet throat boundary-layer removal investigated. Improvements in pressure recovery and distortions by inlet throat bleeding were observed at all Mach numbers and fuselage diverter heights. In general, both inlet critical and peak pressure recoveries increased for an increase in inlet throat bleed area above the no-bleed case. In the range of h/t from 1 to at least 1/3 at Mach numbers 1.8 and 2.0, larger increases in inlet throat bleed area showed decreases in inlet critical pressure recovery, while peak recovery remained nearly constant (fig. 5). At all Mach numbers and fuselage diverter heights, total-pressure distortions of 8 percent or less were obtained with 0.10 or more combined mass-flow ratio bled and spilled (fig. 4). It is interesting to note that except for the pressure distortions at Mach number 2.0 and $h/t = 1$, diffuser pressure recoveries and distortions of the bleed configuration with no mass flow bled (open circles, fig. 4) were as good as or better than those for the smooth-contour diffuser (solid symbols, fig. 4). The greatest improvement of the bleed configuration over the smooth-contour diffuser was noted in the range of h/t values of 2/3 and 1/3.

Cross plots of the variation of peak pressure recovery with the ratio of internal-bleed minimum exit area to inlet throat area are presented in figure 5. Maximum pressure recoveries at Mach number 2.0 were about 0.91 and at each Mach number appeared comparable for all external diverter heights, provided sufficient bleed area was available. An extrapolation of the curves of figure 5 is required to illustrate this point for the fuselage diverter height of 0. Confidence for such an extrapolation is offered by unpublished data for an internal ram scoop located at the inlet throat of the model. This ram scoop, which was opened to permit greater bleed mass flows, showed total-pressure recoveries up to 0.91 at Mach number 2.0 for the fuselage diverter height of 0. This relative insensitivity of the inlet peak pressure recovery to variations in fuselage diverter height indicates little necessity to use a conservative h/t in the design of supersonic inlet installations employing inlet throat bleed. However, the relative sensitivity of the smooth-contour diffuser to a decreasing h/t down to 1/3 may again be noted in figure 5.

The critical main-duct mass-flow ratio for no internal bleed decreases with decreasing fuselage diverter height (fig. 4). This mass-flow reduction was compared with the theoretical mass-flow decrement in a boundary layer with a 1/7-power velocity ratio profile. The boundary-layer profile measured with the survey rake ahead of the inlet agreed very well with the 1/7-power-law profile. At Mach numbers 2.0 and 1.8, the critical mass-flow-ratio reduction with no internal bleed was greater than that predicted by the boundary-layer decrement alone. The additional

spillage occurred behind the ramp oblique shock. At h/t values of 2/3 and 1/3 this additional spillage mass-flow ratio was about 0.01, but increased to 0.05 at $h/t = 0$.

Data generally were taken over a range of mass flows down to the minimum stable main-duct mass-flow ratio. The minimum stable mass-flow ratio was determined by simultaneous observation of shock oscillation and diffuser static-pressure fluctuation. Occasionally, however, additional data were taken in the pulsing regions of the inlet. These data are indicated by the tailed points in figure 4. The numerals adjacent to the tailed points on the pressure-recovery - mass-flow plots (fig. 4) indicate the total amplitude of pulses (1 to 3 percent) to the nearest percent of diffuser total pressure. It is possible that because of these small pulse amplitudes, the minimum stable mass-flow ratios indicated may not necessarily represent practical operating limits.

From the variation of drag coefficients shown in figure 4, it is seen that the minimum drag decreased for decreasing fuselage diverter height. By eliminating the fuselage diverter ($h/t = 0$), the minimum drag was reduced by about 25 percent of the minimum drag at $h/t = 1$. The drag rise for bleeding through the internal-bleed system (differences between minimum drag coefficients at successive ratios of internal-bleed minimum exit area to inlet throat area $\frac{A_{B,e}}{A_t}$) was generally close to the subcritical drag rise (for the same amount of mass-flow spillage behind the normal shock) at Mach number 2.0, although less than that at the lower Mach numbers. This drag penalty for inlet throat bleeding is greater than that assumed in the calculations presented in references 4 and 5, although it is believed that the bleed system used in this investigation could be improved and the drag reduced. Net gains in thrust minus drag comparable to those of the two references will nevertheless be shown in subsequent figures. These gains may possibly be due to a lower additive drag rise for the subject model.

The inlet-engine thrust-minus-drag values were computed to determine the over-all performance of the several combinations of boundary-layer removal. Thrusts were obtained for a typical turbojet engine assumed to be operating at 35,000 feet with maximum afterburning. At each Mach number, the inlet and engine were matched over the mass-flow range for each configuration (each combination of diverter height and bleed area), and the maximum thrust minus incremental drag of each configuration is presented in figure 6(a) as a percent of the maximum thrust of the basic configuration. The basic configuration is defined as the inlet with no internal bleed (bleed exit closed) at an external diverter height equal to the fuselage boundary-layer thickness ($h/t = 1$). External drag coefficients and model frontal area were assumed to remain constant for changes in inlet size required to accommodate changes in diffuser weight flow (see refs. 4 and 5) for the curves of figure 6(a) and the solid curves of figure 6(b).

Net gains in available thrust by bleeding internally were shown at all Mach numbers and fuselage diverter heights. With sufficient bleed area, the available thrust at any Mach number and fuselage diverter height was improved over the thrust of the basic configuration. For $h/t = 1$ down to $h/t = 1/3$ it would appear that, for a fixed bleed, a bleed minimum area of 15 to 20 percent of the inlet throat area would be optimum over the Mach number range investigated. The variations of available thrust for the inlet with the smooth-contour diffuser, the bleed passage closed at its exit, and the optimum-bleed (maximum thrust minus drag) configuration at each fuselage diverter height are presented in figure 6(b). The sensitivity of the smooth-contour diffuser to submersion in the boundary layer is contrasted with the relative insensitivity of the inlet with the bleed exit closed. The maximum thrust minus drag (optimum bleed) at $h/t = 0$ and Mach number 2.0 is not indicated in figure 6(b) since it appeared that this condition was not obtained with the inlet throat bleed areas investigated.

Conservative estimates of the maximum gains in available thrust for the conditions of optimum internal bleed are shown by the dash-dot lines of figure 6(b). In the computation of these thrusts, it was assumed that the external drag coefficients remained constant and that the model frontal area varied in proportion to the changes in inlet size required to accommodate changes in diffuser weight flow. Thus, optimum combinations of fuselage and inlet throat boundary-layer removal showed gains in available thrust from 3 to 10 percent over the case of no inlet throat bleed at $h/t = 1$ (fig. 6(b)). Optimum combinations of the two methods employed fuselage diverter heights in the region from zero to one-third of the fuselage boundary-layer thickness. Pressure distortions at maximum net thrust (optimum inlet throat bleed) were below 10 percent at each Mach number and fuselage diverter height.

The additional use of an internal-bleed removal system increases the number of ways in which air is spilled, diverted, or bypassed in and around an inlet-diffuser installation. The paths of primary interest in this discussion are those taken by (1) the fuselage boundary-layer mass flow diverted by the fuselage diverter system, (2) the mass flow spilled through the inlet throat bleed system, (3) the mass flow spilled behind the inlet normal shock through subcritical operation of the inlet, and (4) the mass flow spilled behind the ramp oblique shock as affected by changes in the fuselage diverter height. The maximum thrust-minus-incremental-drags of each fuselage diverter height, and the corresponding pressure recoveries and drag coefficients, are plotted in figure 7 against the gross mass flow spilled (sum of steps (1) to (4) previously mentioned) from the critical mass-flow ratio at $h/t = 1$ and no inlet throat bleed. The minimum gross mass flow spilled at each fuselage diverter height is the sum of steps (1) and (4). The mass flow described in step (1) was computed for a boundary layer with a 1/7-power velocity ratio profile.

The variations in pressure recovery and drag imply the resulting variation in the available thrust ratio. It should be noted that identical thrusts obtained at lower gross mass flows spilled are done so with correspondingly smaller model frontal areas and that identical thrusts obtained at lower drags will permit reductions in specific fuel consumption. It would then appear from figure 7 that optimization of net thrust and specific fuel consumption could favor fuselage diverter heights in the range from zero to one-third of the boundary-layer thickness for some supersonic inlet installations employing inlet throat bleed. Although net thrusts were highest for the fuselage diverter height of zero at Mach number 1.5, this diverter height loses its attractiveness at the higher Mach numbers.

SUMMARY OF RESULTS

An experimental investigation to evaluate combinations of fuselage and inlet throat boundary-layer removal for a ramp-type side inlet was conducted in the Lewis 8- by 6-foot supersonic wind tunnel at Mach numbers 1.5, 1.8, and 2.0. The following results were obtained:

1. Optimum combinations of fuselage and inlet throat boundary-layer removal showed gains in available thrust from 3 to 10 percent over the case of no inlet throat bleed and full external fuselage boundary-layer removal. The maximum gains occurred with fuselage boundary-layer diverter heights from zero to one-third of the boundary-layer thickness.

2. Maximum pressure recoveries at Mach number 2.0 were about 0.91 and at each Mach number appeared comparable for all fuselage diverter heights, provided sufficient bleed area was available.

3. Pressure distortions at maximum net thrusts were below 10 percent at each Mach number and diverter height.

Lewis Flight Propulsion Laboratory
National Advisory Committee for Aeronautics
Cleveland, Ohio, January 23, 1956

REFERENCES

1. Goelzer, H. Fred, and Cortright, Edgar M., Jr.: Investigation at Mach Number 1.88 of Half of a Conical-Spike Diffuser Mounted as a Side Inlet with Boundary-Layer Control. NACA RM E51G06, 1951.

2. Weinstein, M. I.: Performance of Supersonic Scoop Inlets. NACA RM E52A22, 1952.

3. Valerino, Alfred S., Pennington, Donald B., and Vargo, Donald J.: Effect of Circumferential Location on Angle of Attack Performance of Twin Half-Conical Scoop-Type Inlets Mounted Symmetrically on the RM-10 Body of Revolution. NACA RM E53G09, 1953.

4. Campbell, Robert C.: Performance of a Supersonic Ramp Inlet with Internal Boundary-Layer Scoop. NACA RM E54I01, 1954.

5. Obery, Leonard J., and Cubbison, Robert W.: Effectiveness of Boundary-Layer Removal Near Throat of Ramp-Type Side Inlet at Free-Stream Mach Number 2.0. NACA RM E54I14, 1954.

6. Piercy, Thomas G.: Preliminary Investigation of Some Internal Boundary-Layer-Control Systems on a Side Inlet at Mach Number 2.96. NACA RM E54K01, 1955.

[redacted]

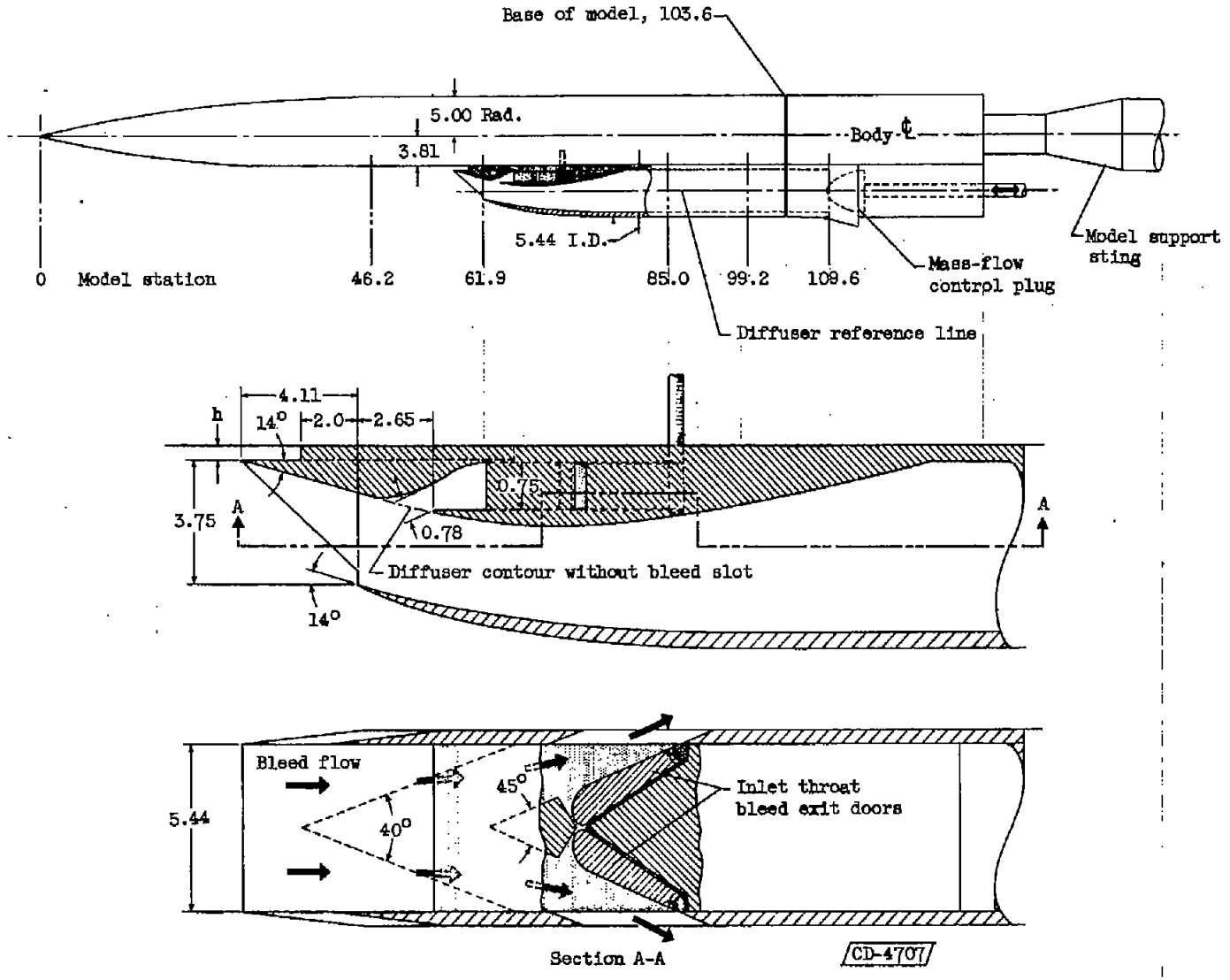

Figure 1. - Schematic drawing of model and inlet. All dimensions in inches.

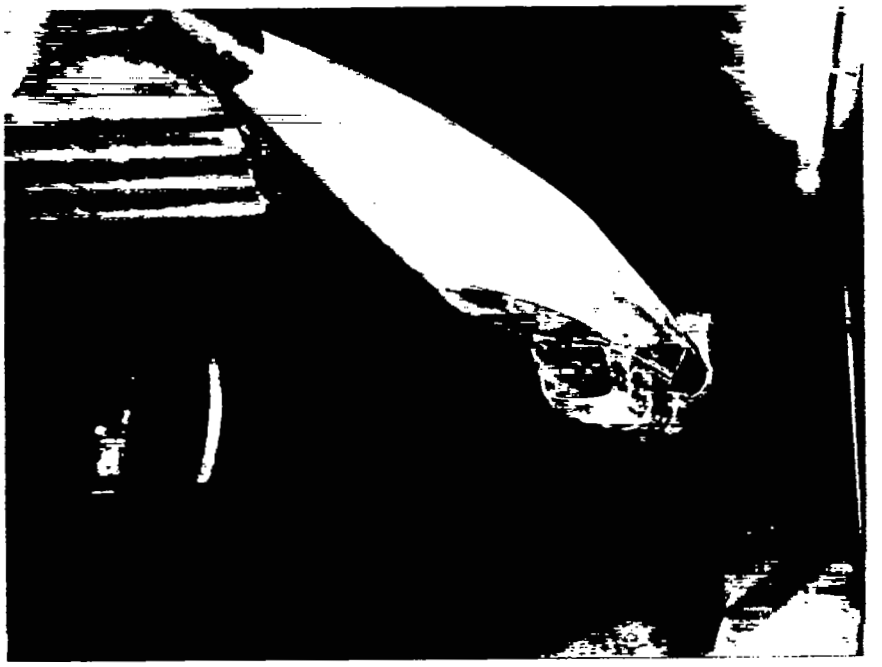

(a) Model installed in 8- by 6-foot supersonic wind tunnel.

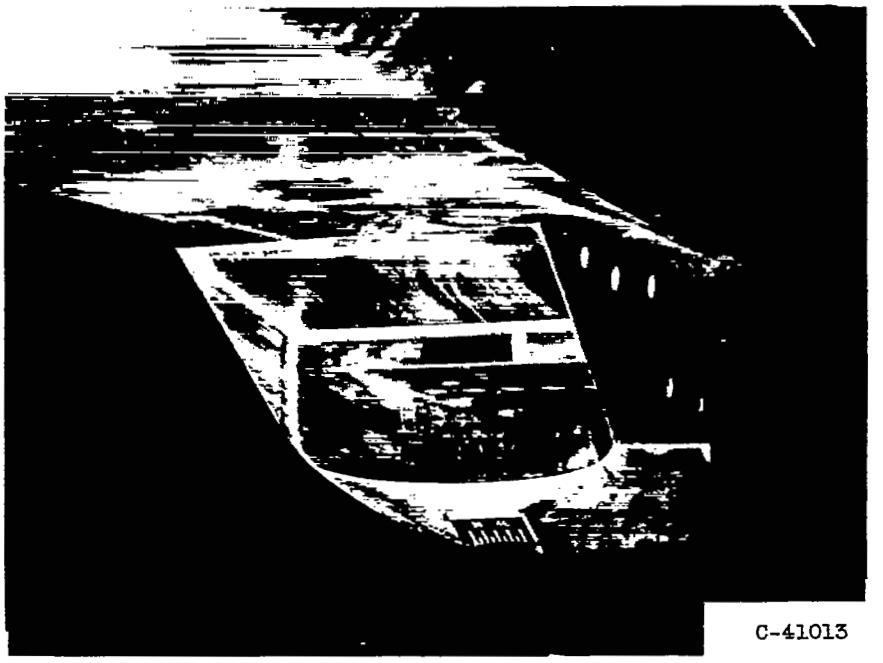

(b) Close-up of model inlet and internal flush bleed.

Figure 2. - Photographs of model.

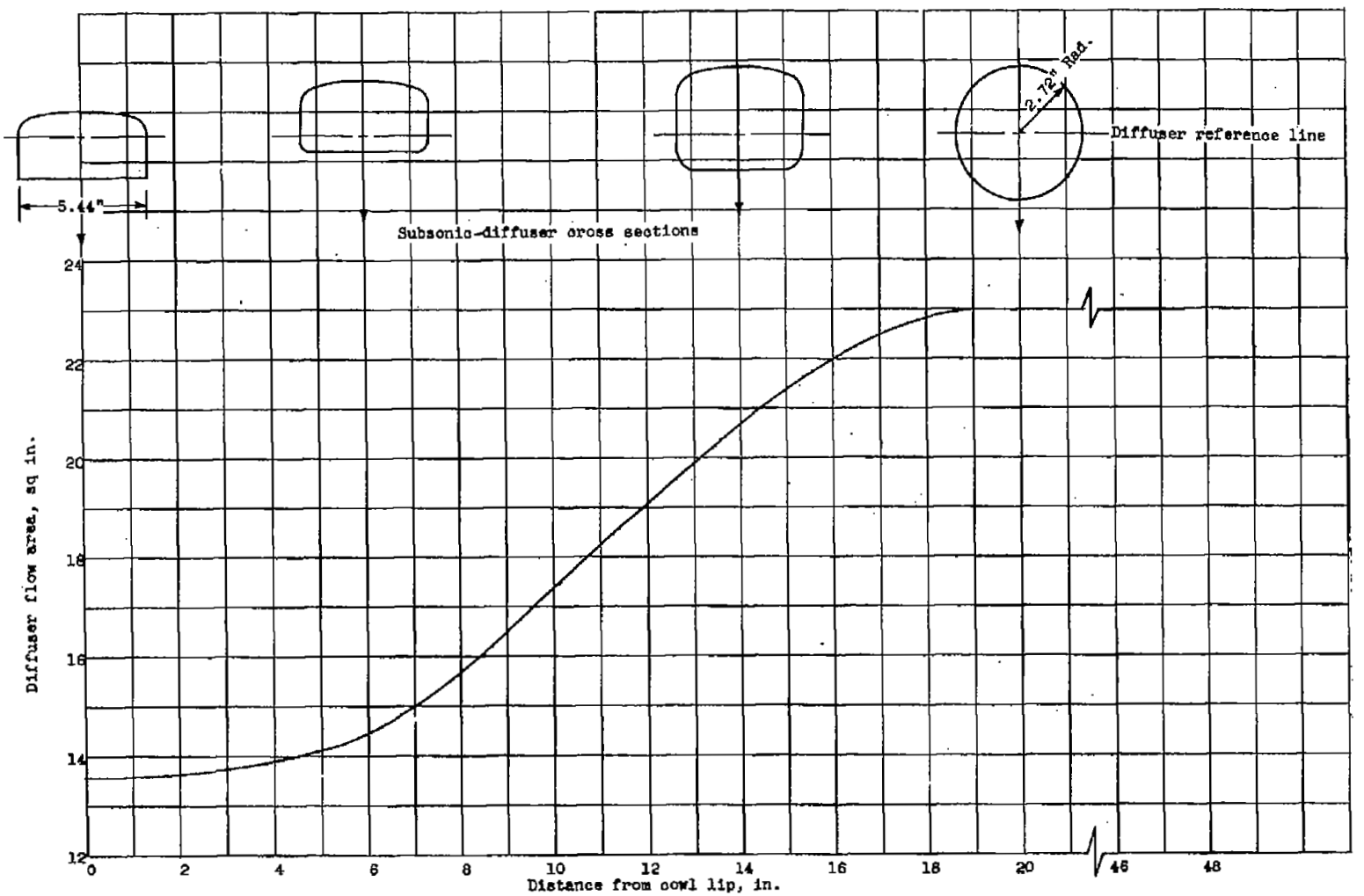

Figure 3. - Subsonic-diffuser area variation. Inlet throat hydraulic diameter, 3.52 inches.

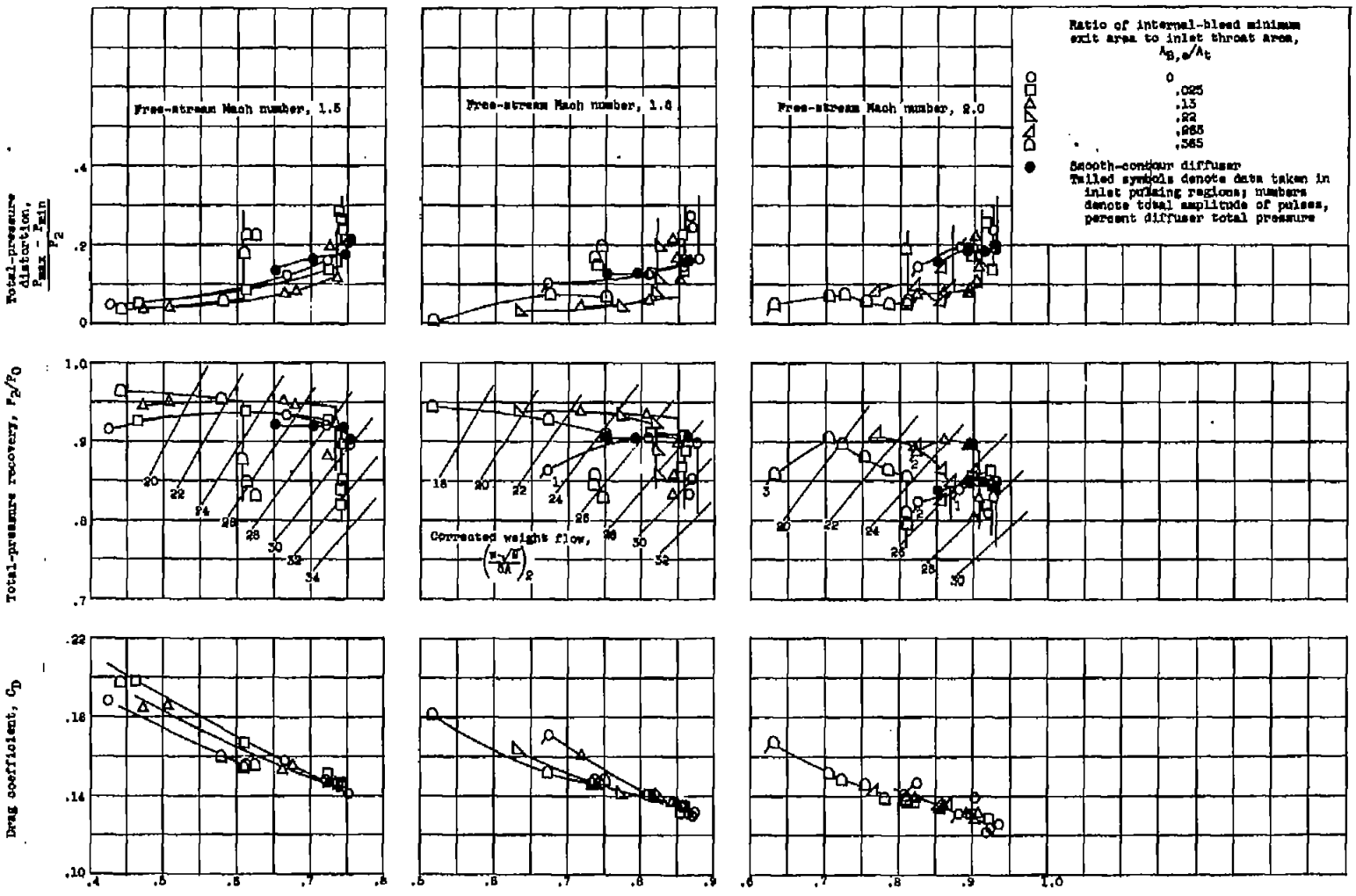

(a) Fuselage diverter height parameter, h/t, 1.

Figure 4. - Effect of inlet throat bleed on inlet performance.

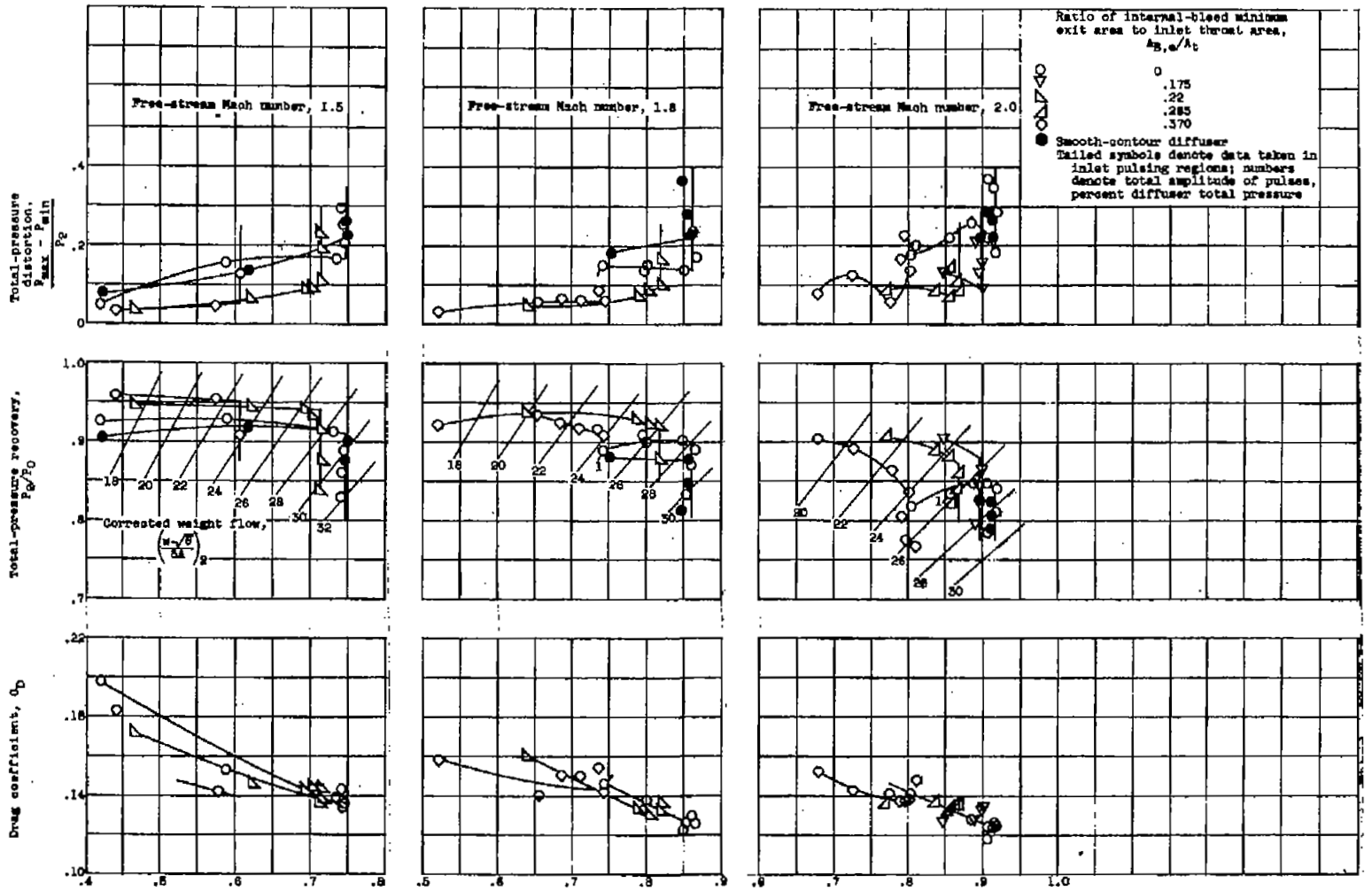

(b) Fuselage diverter height parameter, h/t, 2/3.

Figure 4. - Continued. Effect of inlet throat bleed on inlet performance.

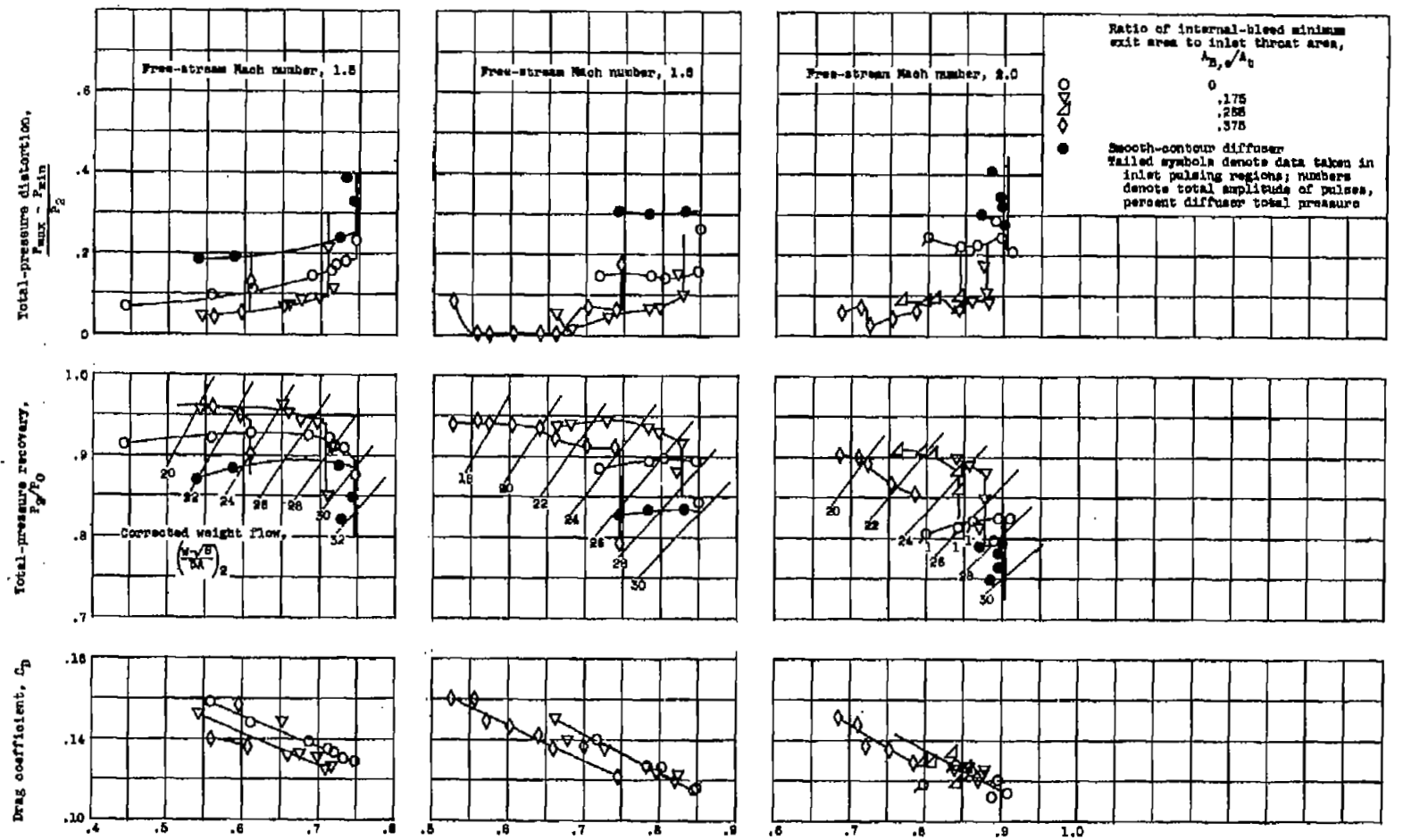

(c) Fuselage diverter height parameter, h/t, 1/3.

Figure 4. - Continued. Effect of inlet throat bleed on inlet performance.

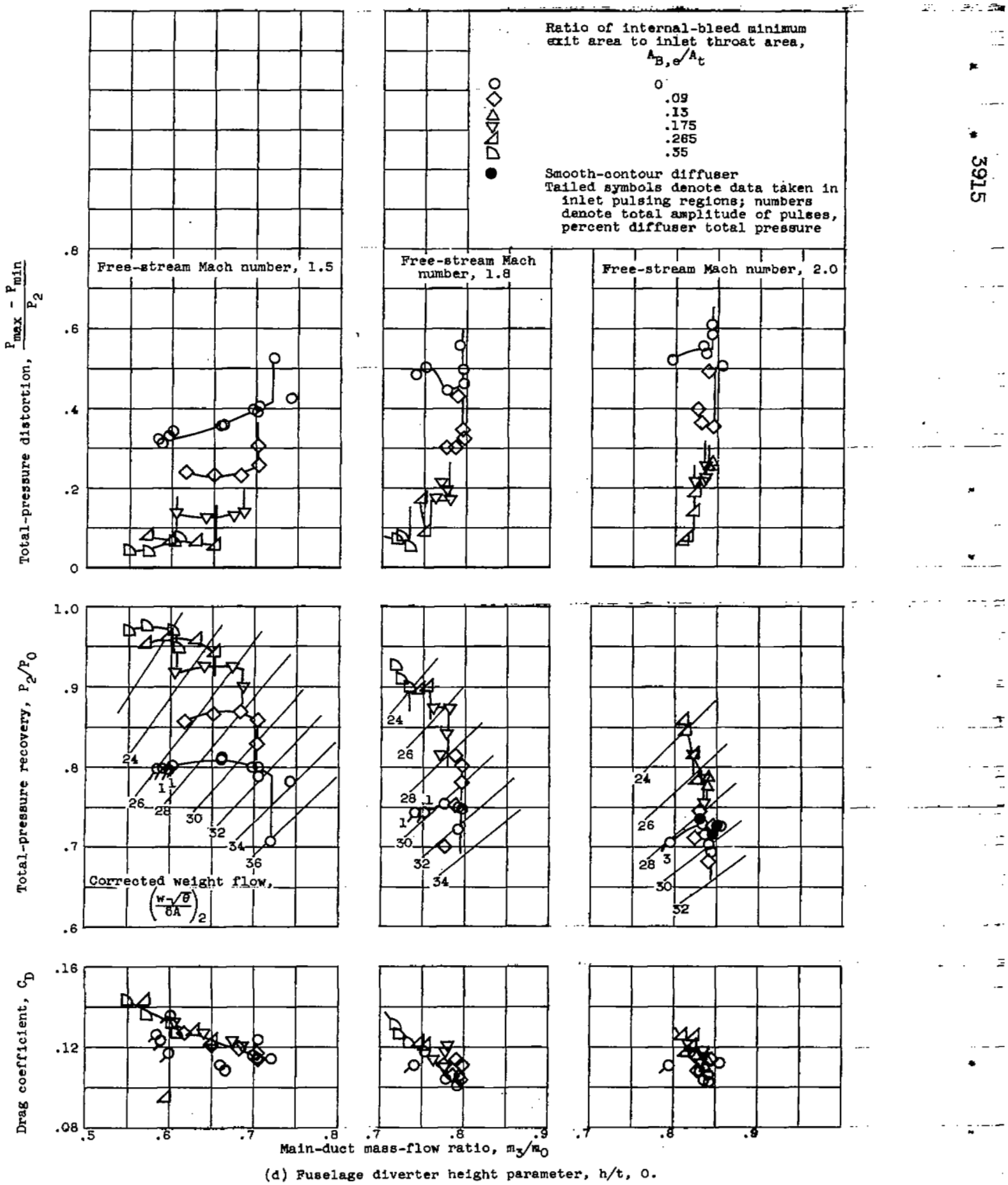

(d) Fuselage diverter height parameter, h/t, 0.

Figure 4. - Concluded. Effect of inlet throat bleed on inlet performance.

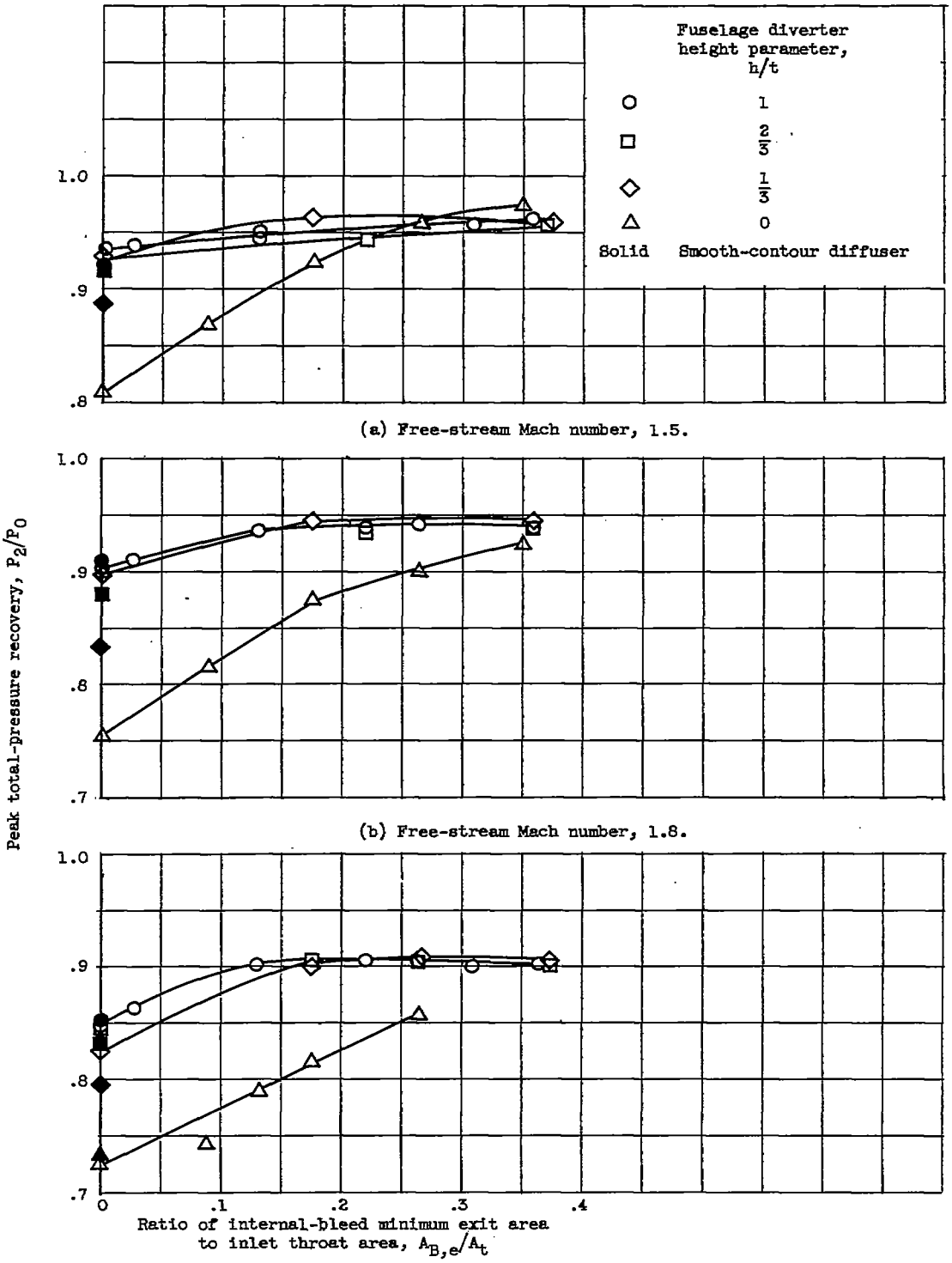

(a) Free-stream Mach number, 1.5.

(b) Free-stream Mach number, 1.8.

(c) Free-stream Mach number, 2.0.

Figure 5. - Inlet peak pressure recovery.

[redacted]

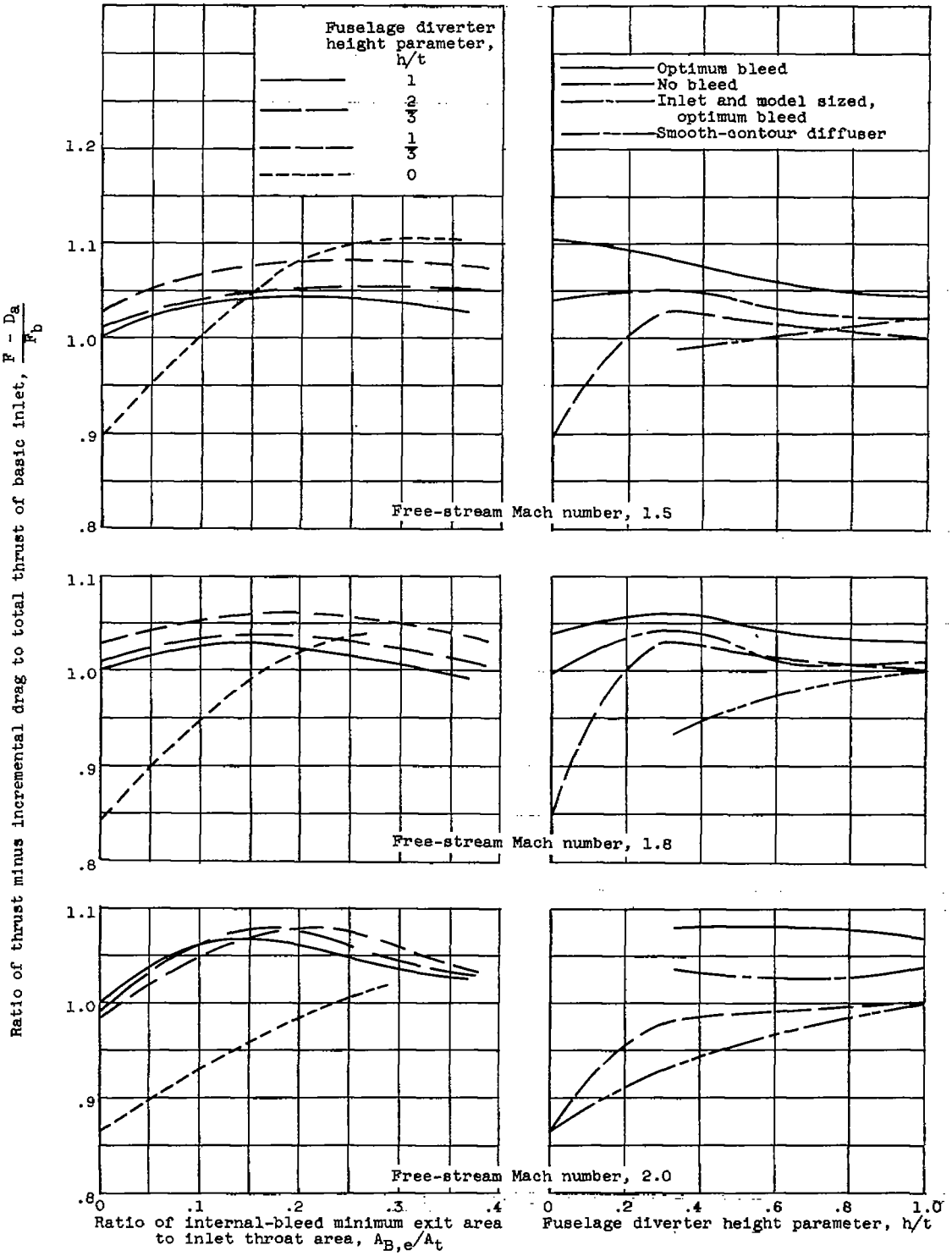

(a) Effect of internal-bleed area. (b) Effect of fuselage diverter height.

Figure 6. - Thrust parameter for combinations of boundary-layer removal.

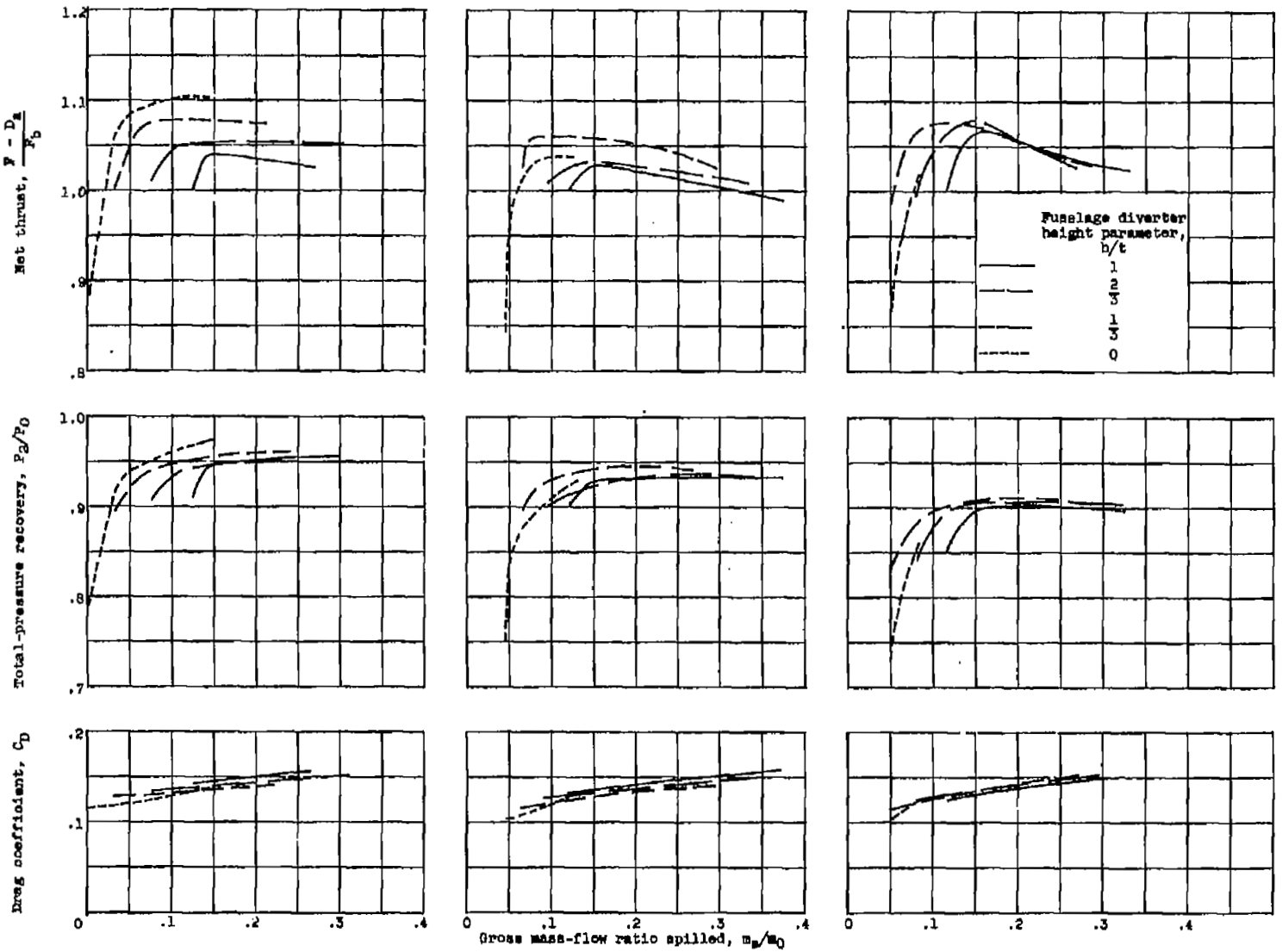

(a) Free-stream Mach number, 1.5. (b) Free-stream Mach number, 1.8. (c) Free-stream Mach number, 2.0.

Figure 7. - Effect of gross mass flow spilled on performance parameters.